Phase correction for the BIMA array: atmospherical model calculations for the design of a prototype correlation radiometer

J. Staguhn[a], A.I. Harris[a], R.L. Plambeck[b], and W.J. Welch[b]

[a]Astronomy Department, University of Maryland, College Park, 20742, USA
[b]Astronomy Department, University of California, Berkeley, CA 94720, USA

To appear in the Proceedings of SPIE's International Symposium on Astronomical Telescopes and Instrumentation

Phase correction for the BIMA array: atmospherical model calculations for the design of a prototype correlation radiometer

J. Staguhn[a], A.I. Harris[a], R.L. Plambeck[b], and W.J. Welch[b]

[a]Astronomy Department, University of Maryland, College Park, 20742, USA

[b]Astronomy Department, University of California, Berkeley, CA 94720, USA

ABSTRACT

We present results from atmospheric model calculations for the design of an atmospheric phase correlation radiometer for the Berkeley-Illinois-Maryland Millimeter Array (BIMA). The radiometer will monitor the atmospheric path delay by observing the fluctuations in the emission from tropospheric water vapor which causes de-correlation of astronomical signals which are observed along different lines of sight. We discuss the applicability of monitoring the optically thick 183 GHz water line and the optically thin 22 GHz water line. We conclude that for the BIMA site, which is not extremely dry, optical depth effects make observations of the 183 GHz line unfavorable. We discuss possible observing schemes and conclude that a multi-channel radiometer provides the highest achievable accuracy, as it provides the possibility to fit a line shape model to the observed channels. Systematic errors due to the unknown altitude distribution of water vapor and optical depth effects can be significantly reduced by this scheme, compared to methods which only monitor the change of the peak brightness temperature of the water vapor line.

Keywords: Phase correction, radio astronomy, interferometry, radiometers, correlators

1. INTRODUCTION

At mm/sub-mm wavelengths phase fluctuations are predominantly caused by line of sight fluctuations in the amount of atmospheric precipitable water vapor (pwv). There is a linear relation between the amount of precipitable water vapor and the delay length (L) for the radiation, independent of frequency (no dispersion) in the cm to sub-mm regime. This means that dL/d(pwv) is a constant over the frequency range discussed in this paper. Under "normal" temperatures and pressures the water vapor dependent delay term can be approximated by (Thompson, Moran & Swenson, 1994):

$$L[\mathrm{cm}] = 0.228\mathrm{P}_0[\mathrm{mbar}] + 6.3\mathrm{pwv}\ [\mathrm{cm}], \tag{1}$$

where P_0 is the pressure at the surface. The water vapor content of the atmosphere cannot be measured directly, but, for our purposes, it can be approximately derived from the brightness of the sky emission. The relation between the observed sky brightness temperature and the amount of pwv is complicated by the following effects:

a) Line brightness temperatures depend on both pressure and the physical temperature in the emitting region. Thus the line brightness temperature depends on the altitude of the emitting layer. Line shapes of tropospheric water vapor in the cm- and mm regime are well described by the kinetic

Other author information: E-mail: staguhn@astro.umd.edu, harris@astro.umd.edu, plambeck@astron.berkeley.edu, welch@jack.berkeley.edu

line shape theory, but the theory breaks down far from the line centers. The "continuum" between lines has to be approximated by an empirical formula.

b) Optical depth effects have to be taken into account, especially for the strong 183 GHz water line.

c) The observed sky temperature is not only from emission of water vapor. For the frequency ranges discussed in the following, it is sufficient to assume that the emission of most atmospheric molecules is constant and thus can be ignored for our purposes. Nevertheless water dimers and water droplets add a fluctuating amount of "excess absorption" which possibly cannot be ignored at all frequencies as discussed in the following, especially, if observations are made far off the line centers of the observable water lines.

d) The antenna picks up ground emission from antenna spillover.

In order to derive a scheme for a phase monitor, which is most insensitive to the effects described above, we made atmospherical model calculations. Our initial aim was to determine the path length difference for the lines of sight of 2 telescopes to an accuracy of at most 18 degrees phase error (1/20th of a wavelength). This path difference for the signals in the 2 telescope beams corresponds to 10% loss of signal due to de-correlation ($\sin^2(18^o)$). To achieve this accuracy for observations at 1mm wavelength, we need to measure path length delays of 50 μm / $\sqrt{2}$ = 35 μm rms with each antenna. These are the numbers we will discuss in the following.

2. LINE SHAPES

In the troposphere the dominant line broadening mechanism is collisional excitation. Doppler (or thermal) broadening is only important at altitudes above 70 km. Collisional (or pressure) line broadening is described by the line shape theory of Ben Reuven. By assuming that no momentum reversing collisions happen and that all phase changes are equally probable, the Ben Reuven line shape simplifies to the Van Vleck-Weisskopf line shape. Assuming only momentum reversing collisions instead, the Ben Reuven line shape turns into the kinetic line shape introduced by Gross (equation 2.3.12 in Waters, 1976).

In the cm- and mm-regime, the observed telluric line shapes are best fit by the kinetic line shape theory. Nevertheless the kinetic line shape theory fails to describe the emission far off (i.e. significantly further off than the half power points) the line centers. There is an additional component of "excess emission" observed. It is not yet proven, whether this excess is due to an insufficient physical description of the collisional line broadening in the kinetic line shape theory, or due to an atmospheric component (such as water dimers), which is somehow proportional to the water vapor density (but might depend also on the absolute humidity), and which is not included in the models. An empirical formula for this "continuum" offset is given in equation 2.3.22 in Waters (1976). This absorption coefficient, which scales as ν^2, appears to well reproduce observations up to several hundred GHz. Nevertheless this fit is unphysical and it is unlikely to describe the actual "excess emission" under all weather conditions.

3. MODEL CALCULATIONS

In the following we will discuss possible options for water vapor monitoring. We will be assuming that the altitude distribution of an additional layer of water vapor, which produces the phase noise we aim to monitor, may be anywhere between the telescope and 3000 m above (which includes the range of most turbulence in the amount of pwv (Waters 1976)).

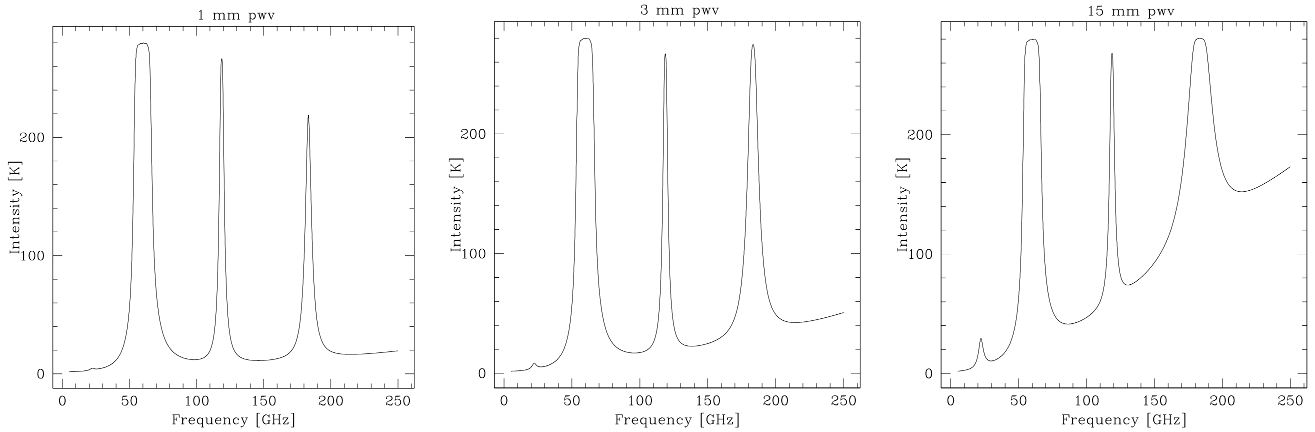

Figure 1. Sky brightness temperature at 1 km altitude for 1mm, 3mm, and 15mm pwv.

3.1. The code used for the calculations

The code used for the calculations is based on the equations given in Waters (1976): the kinetic line shape is used for the water vapor and oxygen lines, including the corresponding line width parameters; additionally the equation for the $\propto \nu^2$ excess emission from the same article was used. For atmospheric layers of 10 m thickness radiation transfer effects, as well as pressure and temperature effects, are calculated. The vertical temperature- and pressure structure of the atmosphere is taken from the US 1964 standard atmosphere (McClatchey et al., 1972). A site altitude of 1 km was used for all calculations.

3.2. Results of model calculations

Fig. 1 shows the sky brightness temperature between 5 and 250 GHz for a) 1mm, b) 3mm, and c) 15mm pwv for a mid-latitude site at 1 km altitude. The two major oxygen lines at 60 GHz and around 119 GHz are optically thick. The water line at 22 GHz is optically thin, even at 15 mm pwv, whereas the 183 GHz line becomes optically thick for pwv columns of greater than 1 mm.

Path length fluctuations in the mm regime are caused by the fluctuations in the water vapor; these fluctuations also show up as changes in sky brightness temperature. We present simulations for 4 frequency intervals, calculated for total pwv columns: 0.1 mm, 1 mm, 3 mm, and 15 mm. Fig. 2 presents plots of the change in sky brightness temperature, caused by an extra layer of water vapor which produces an additional phase delay of 35 μm. The five lines in each frame correspond to water vapor at different altitudes above the telescope. The altitudes are spaced by 500 m. The lowest layer is 500 m above the telescope.

The dependence of sky brightness change on the altitude of the additional layer of water vapor reflects the temperature and pressure dependence of the line shapes, plus optical depth effects (which dominate the change in sky brightness of the 183 GHz line). The line shape effect cancels at the so-called hinge points where the level of emission is independent of the altitude. Nevertheless for higher optical depths the hinge points vanish; even at 1mm pwv the 183 GHz "line" has no hinge points.

A major problem with observations in the continuum around 85 GHz and between 220 and 230 GHz can be seen in Figs. 2 and 3: The sky brightness for a certain amount of additional water vapor depends relatively strong on the additional component's altitude. The relative uncertainty (i.e. mean emission level at a given frequency versus uncertainty in this intensity) introduced by

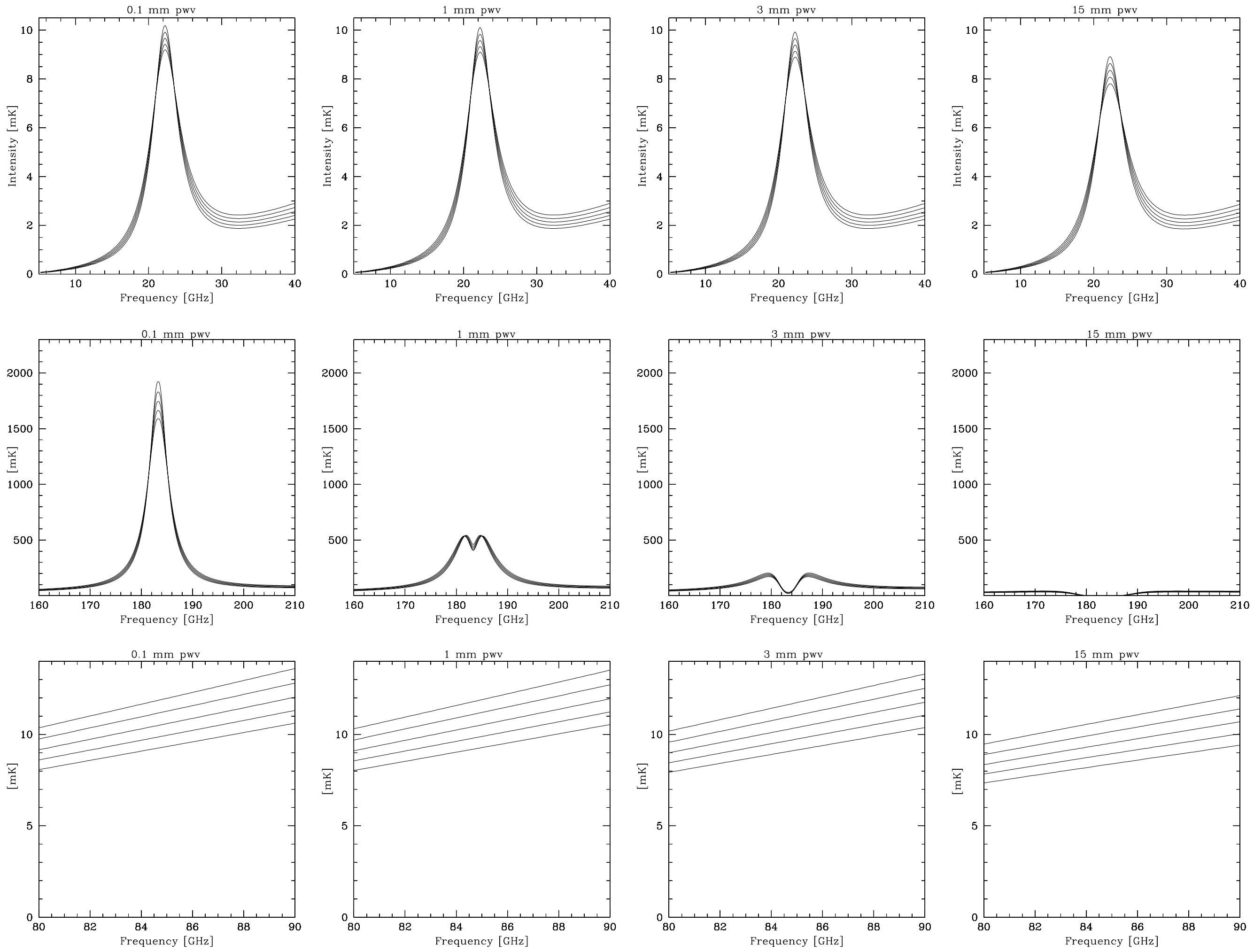

Figure 2. Change in sky brightness temperature, caused by an additional layer of water vapor which causes a phase delay of 35 μm for different absolute values of pwv, as stated in the figure. Note that the line center of the 185 GHz line suffers optical depth effects even at 0.1 mm total amount of pwv. The five lines shown in each plot correspond to the water vapor, distributed at different altitude layers above the telescope. The layers are spaced by 500 m with a starting value of 500m above the telescope.

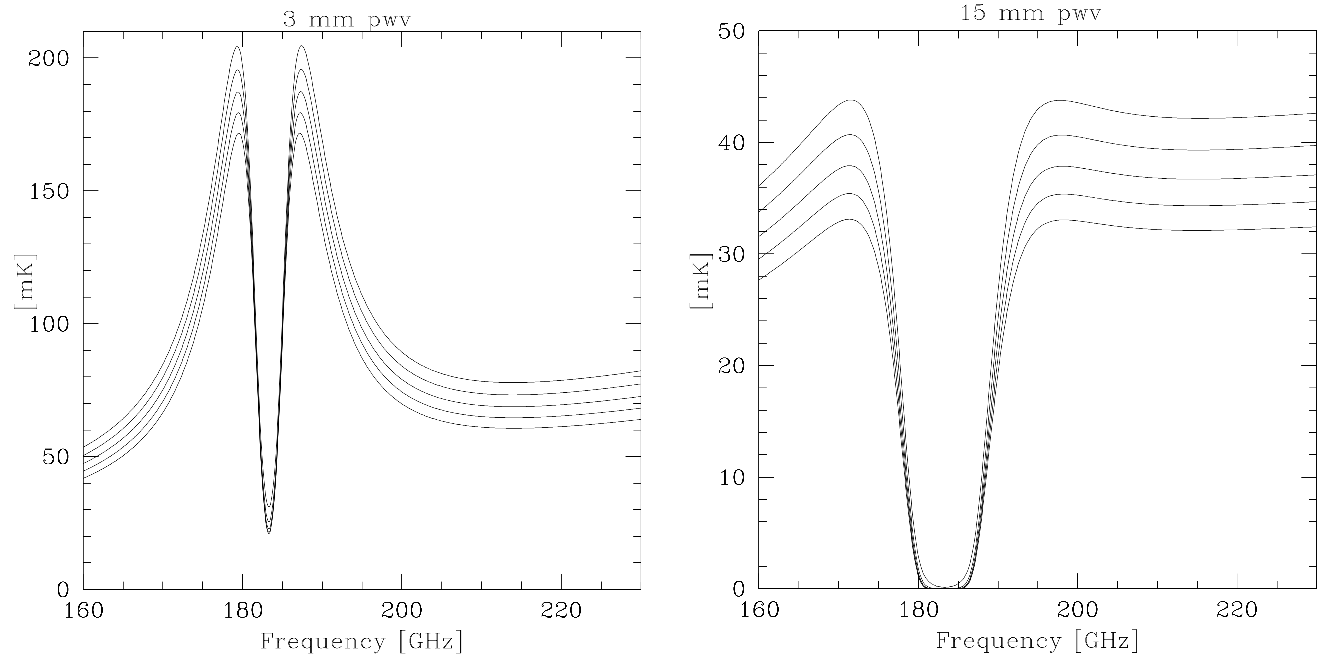

Figure 3. Change in sky brightness temperature, due to an extra layer of water vapor which causes an additional phase delay of 35 μm for different absolute values of pwv, as stated in the figure. The five lines shown in all plots corresponds to water vapor layers at different altitudes above the telescope. The layers are spaced by 500 m, the lowest layer is 500 m above the telescope.

an unknown altitude is about 30% at all frequencies and ranges of total pwv shown in the figures. Monitoring phase fluctuations by observing the total power of the continuum has the disadvantage that it is not possible to derive the altitude distribution of the water vapor. Additionally the continuum emission is stronger dominated by emission from molecules other than water vapor than the emission near the center of water vapor lines.

Fig. 2 demonstrates that even at 1 mm pwv optical depth effects dominate the line shape of the 183 GHz line. Figure 3 shows the change in the 183 GHz line emission and the continuum up to 230 GHz for pwv columns of 3 mm and 15 mm in detail. The figure demonstrates the strong optical depth effects and the dependence of the change in sky brightness on the altitude of the water vapor. At 15 mm pwv, which can occur in summer at the BIMA site Hat Creek, the 183 GHz line is optically so thick that its difference signal is weaker than that of the continuum between the lines.

At 22 GHz the altitude dependent differences of about 10% near the line center (see Figure 2) and the differences in the line wings are almost independent of the absolute amount of pwv; only above 10 mm pwv optical depth affects the peak temperature of the line slightly. This is an important property of the 22 GHz line which will be discussed in more detail in the next section.

The disadvantage of observing the 22 GHz line is that the change of brightness of this line is relatively weak. The 183 GHz line shows a change of sky brightness a factor of 20 (at 1 mm pwv) to 100 (in the extreme optically thin case) times more that of the 22 GHz line.

4. IN SEARCH FOR A GOOD "OBSERVABLE"

Due to its optical depth (typical values of the pwv at Hat Creek range between 1 mm and 15 mm pwv) the 183 GHz line is not suitable for a water vapor radiometer at Hat Creek. We will thus focus on the requirements for a radiometer for the optically thin 22 GHz water vapor line.

The goal of our calculations is to specify what measurements are best suited to monitor the fluctuations of the water vapor in the atmosphere above the telescope. In order to simulate the sky emission for a given change of water vapor, we calculated an ensemble of synthetic spectra for a certain amount of water vapor. The data for the line shapes were synthesized following the equations in Waters (1972) (see previous section). Each spectrum in this ensemble has an at random chosen value for the altitude of the additional amount of water vapor. The range of these altitudes goes from 500 m to 3000 m above ground. Additionally, in a part of the calculations a random value for the total amount of pwv was generated for each synthesized difference, ranging from 1 mm to 15 mm. In the other cases, as will be indicated, the calculations were made for a value of 10 mm total pwv. In order to be insensitive to emission from other sources, we need to be insensitive to additional offsets and frequency dependent emission which comes not from line of sight water vapor. Ground pick up will produce significant offsets. The contribution of e.g. water droplets will have a power law dependence on the frequency (Waters, 1972). We included random offsets in our synthesized data which are represented by up to second order polynomials in frequency. The coefficients for the offsets range between -10 and +10 mK, those of the linear terms from -1 to +1 mK and the coefficients for the quadratic term have random values between -0.02 and +0.02 mK.

The goal is to find a quantity which we call the "observable" which can be derived from (simulated) measurements of a certain number of frequency channels and which fulfills the following conditions: For a fixed amount of additional water vapor, the observable should give the same result for all of the synthesized spectra. In other words, the observable should be insensitivity to the altitude distribution of the water vapor and to optical depth effects. Additionally the observable needs to have a simple monotonic dependence on the total amount of water vapor. In order to test the last constraint for possible observables we calculated a second set of data. The amount of additional water vapor for each of the 100 new synthesized difference spectra was increased consecutively in steps of 35 μm to a maximum of 3.5 mm additional water vapor column in one layer. Again the altitude of this vapor, and in one of two datasets, the total amount of pwv were chosen randomly. We tried two different approaches to find a suitable observable. These will be discussed in the following two sections.

4.1. The observable derived from a linear combination of single channels

In our first approach we searched for a linear combination of the smallest number of channels which yield a good observable. As one has to allow for offsets and at least linear terms in the difference signal, the observable needs to be derived from the minimum of 3 channels. The best observable for 3 channels has the center channel on the peak of the 22 GHz water line and a channel to each side. One subtracts the weighted observed intensity changes in the line wing channels from the center channel intensity. This scheme is being successfully utilized at the Owens Valley observatory OVRO (Marvel & Woody, 1998). However there are limitations to this method as it amplifies the altitude dependence of the difference signal, if the line wing channels extend beyond the hinge points of the observed line. In practice such a channel separation needs to be chosen in order to have a sufficient signal. The altitude dependence of the additional amount of water vapor on the observable is the major cause of the "noise" relation between the observable and the true path length change which can can be seen in Fig. 4. The figure shows the results from calculation in which 2 GHz wide channels centered at 19.2, 22.2, and 25.2 GHz were combined by subtracting the mean of the line-wing channels from the center channel. The abscissa in Fig. 4 is in units of 35 μm phase delay. The error introduced by the altitude dependence of the difference signal is proportional

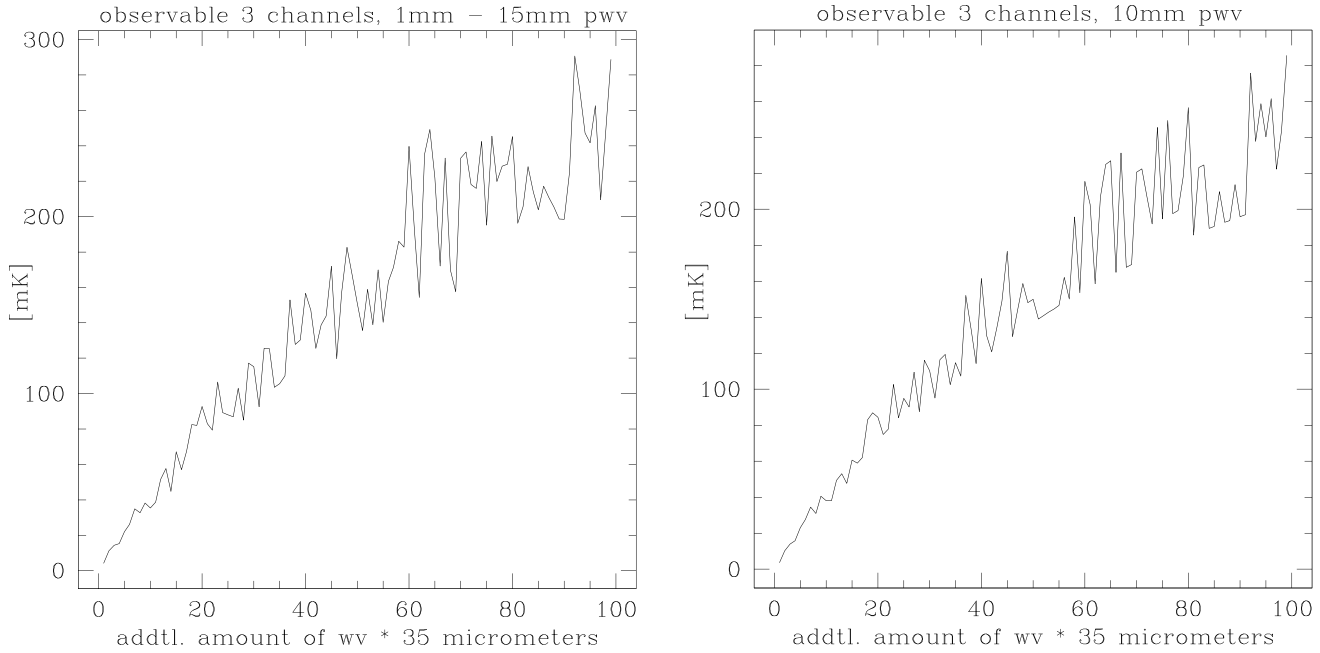

Figure 4. Brightness temperatures of a 3 channel observable with 2 GHz wide channels centered at 19.235, 22.235, and 25.235 GHz. The channels were combined by subtracting the mean of the wing channels from the center channel value. The values of the change in the additional amount of water vapor are indicated on the ordinate. The altitude distribution of the additional water vapor was chosen randomly, as described in the text. The *left frame* shows calculations made for a total amount of pwv chosen randomly between 1 mm and 15 mm for each value of additional water vapor. This value was set constant to 10 mm in the simulation showed in the *right frame.*

to the absolute value for the difference in the signal. Thus the uncertainty in the calculated phase delay is also proportional to the absolute value of the change in phase delay. The right frame in Fig. 4 shows the result of calculations in which the total amount of water vapor was kept constant, whereas in the left frame results are displayed from calculations with random values for the total pwv for each calculated difference, ranging from 1 to 15 mm. The noticeable change in the slope of this observable is caused by optical depth effects produced by the additional amount of water vapor itself. Results from the 3 channel radiometer used for OVRO (Woody, priv. communications) are consistent with this result.

We tried to find a better observable by using a Monte Carlo method for calculating a large number of linear combinations of more than 3 synthesized channel data. Indeed we found observables calculated from more than 3 channels which are less sensitive to altitude- and optical depth effects. However this always comes at the price of a significant decrease in the signal strength of the observable and thus using such observables increases the contribution from the system noise.

4.2. The observable derived from a fit to the line shape

The second approach to finding a good observable is to make line fits to the observed difference spectra. This approach has the advantage that a fit to the line shape does not increase the effective radiometric noise in the result. In the optical thin limit different altitudes of additional vater vapor can, to the first order, be reproduced by only varying the line width parameter in the fitted kinetic line shape to the difference spectrum. This means that the fitted integrated line intensity is to the

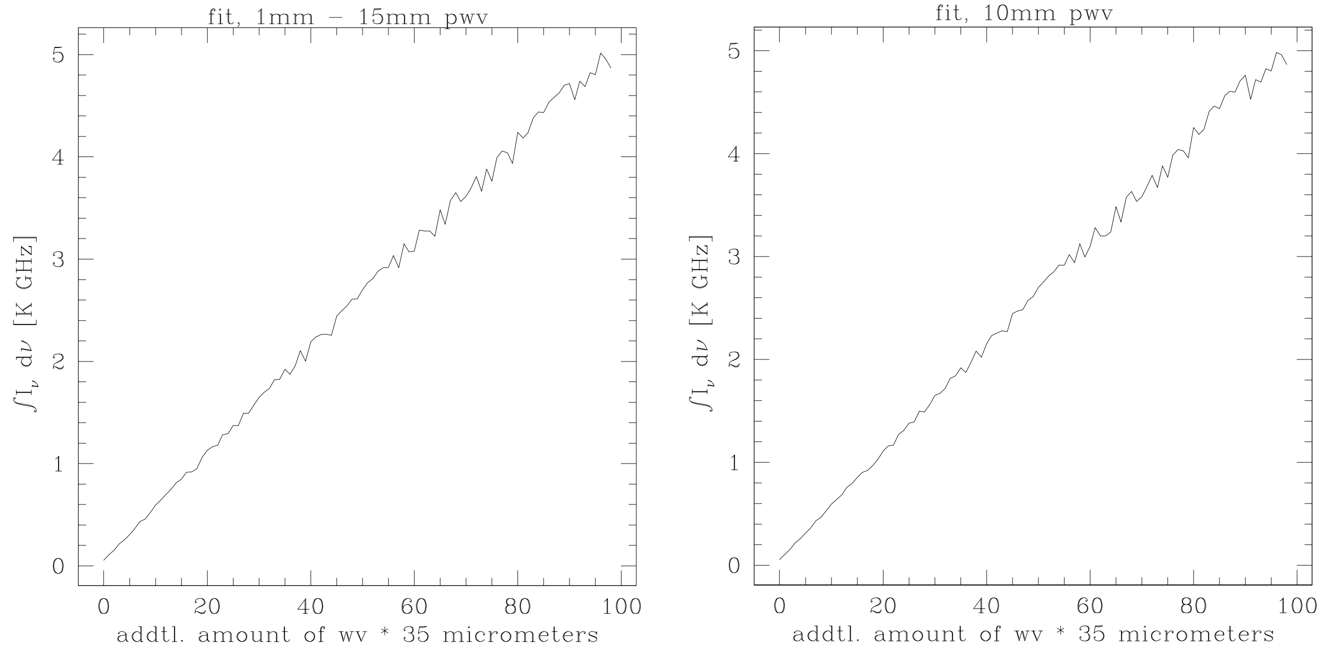

Figure 5. Integrated line intensity of the fitted kinetic line shape to the synthesized dataset of changes in the brightness temperature due to an additional water vapor layer. The values of the change in the additional amount of water vapor are indicated on the ordinate. The fit includes polynomials up to the first order. The number of channels is 32. These are the channels of the radiometer which we plan to build and which is described in the text. The altitude distribution of the additional water vapor was chosen randomly, as described in the text. The *left frame* shows calculations made for a total amount of pwv chosen randomly between 1 mm and 15 mm for each value of additional water vapor. This value was set constant to 10 mm for the simulation seen in the *right frame.*

first order independent of the altitude of the additional water vapor. As was the case for the 3 channel observable, we find that the uncertainty in the phase delay is proportional to the absolute value of the change in sky brightness. The deviation from proportionality in the integrated line intensity of the line also increases with the amount of additional water vapor, but as is the case for altitude effects, on a significantly lower level than for the 3 channel observable. This shows that the fitted integrated line intensity is not only relativelly insensitive to the altitude distribution of the water vapor, but also to moderate optical depth effects. We conclude that the integrated line intensity of the fitted kinetic line shape is a very good observable. In the next section we will discuss the contribution of the radiometer noise.

4.3. Hardware constraints

Our goal is to achieve a rms accuracy of 35 μm in the prediction of the actual path delay. This path delay translates to about 7 mK differential change of the brightness temperature at the line center for the 22 GHz vapor vapor line. The accuracy of an observable is given by the rms of its residuals to a linear (or higher order polynomial) fit to its expected value. In order to obtain the required accuracy of 35 μm rms path delay from the 3 channel observable presented before, an accuracy of 3 mK rms is required. The accuracy requirement for the fitted integrated intensity of the kinetic line shape, which is shown in in Fig. 5, is about 50 mK·GHz rms. We will now discuss the achievable accuracy for the BIMA phase monitor radiometer if we take into account both, receiver noise, and systematic "noise" due to line shape effects.

The current scheme for our radiometer is a 32 channel lag correlator with sideband separation. In this scheme we will use two 16 channel analog lag correlators from an existing correlator (Harris et al., 1998). The local oscillator (LO) frequency will be centered on the 22 GHz water vapor line, the bandwidth in each sideband will range from 750 MHz to 4 GHz which results in a total bandwidth of 6.5 GHz. Each channel has a reception bandwidth of roughly 200 MHz. Commercially available broad band amplifiers suitable for this frequency range (e.g. Miteq JS4-18002600-16-5P, frequency range 18 - 26 GHz) have typical noise figures around 1.5 dB which corresponds to a noise temperature of 120 K at ambient temperature. If the receivers are cooled, the manufacturer predicts that the noise temperature can be reduced by about a factor of 4. The amplifier will be the major source of noise of the receiver. At 22 GHz the sky temperature does not exceed 30 K in the line center, even at 15 mm pwv. Thus we expect to achieve system temperatures in the order of 150 K for an uncooled radiometer. For a cooled radiometer the achievable system temperature should be significantly better than 100 K.

The rms noise temperature of each radiometer channel is given by

$$T_{\rm rms} = \frac{\sqrt{2} \cdot T_{\rm sys}}{\sqrt{\rm B_{rec} \cdot t_{int}}} \tag{2}$$

where $\rm B_{rec}$ is the reception bandwidth of a single channel.

The shortest integration time will be 10 seconds, as this is the minimum read out time for the astronomical data. We thus expect a rms noise temperature for each of the 32 channels of about 5 mK for an uncooled radiometer and about 2 mK, if the radiometer will be cooled. Figure 6 shows the integrated inensity of the fitted kinetic line shape with a channel noise temperature of 2 mK rms in the left frame and 5 mK rms in the right frame of Fig. 6. Fig. 7 shows the residuals to a linear line fit to the data without noise contribution from the radiometer (the data shown in Fig. 5), and the residuals from a linear line fit applied to the data shown in Fig. 6. One can easily see that for 2 mK rms noise temperature per channel the main noise contribution comes from line shape and optic depth effects. For our observable – the integrated intensity of the fitted kinetic line shape – these effects are smaller than our aimed accuracy for values up to about 2 mm of additional water vapor. The noise temperature of an uncooled radiometer, on the other hand, limits the achievable accuracy significantly over the whole range of water vapor fluctuations shown here. The achievable accuracy for the uncooled radiometer will be slightly less than 35 μm rms, even for a small amount of additional water vapor.

4.4. 22 GHz beam overlap

We are planning to incorporate the radiometer in the secondary focus of the BIMA telescopes and have its beam aligned with the mm main beam. It will be possibly placed in the dewar of the astronomical receivers. Fig. 8 shows the overlap of the telescope beams at 220 GHz and at 22 GHz. Up to altitudes of 3000 m above ground, which is the portion of the atmosphere where the strongest fluctuations are caused by water vapor, the beam waists differ by up to a factor of 2, at 2000 m the difference is 1.5. A possible de-correlation in the amount of additional water vapor in the two beams thus has to be expected for (in terms of our integration time) fast fluctuations in the highest altitude layers.

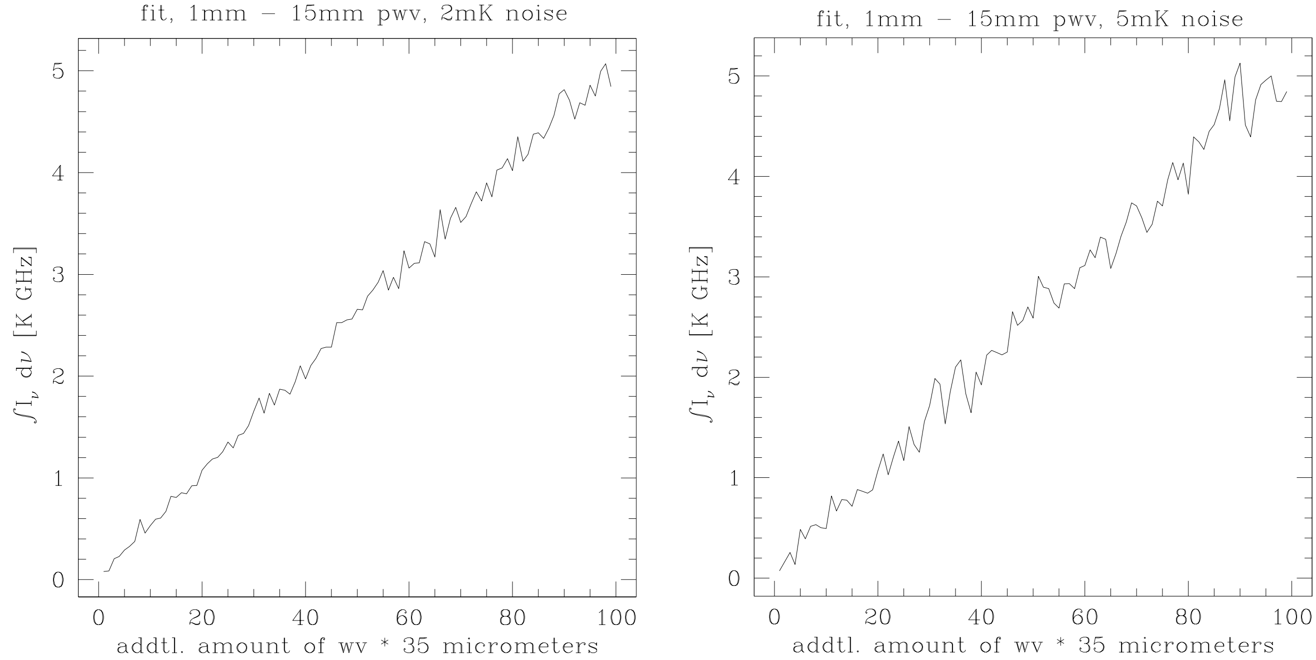

Figure 6. Integrated intensity of the fitted kinetic line shape to the synthesized dataset of change in brightness temperature for an increasing amount of additional water vapor as indicated. The figure shows a fit to the same dataset as shown in the right frame of Fig. 5, but with added channel noise of 2 mK rms *(left)* and 5 mK (*right*).

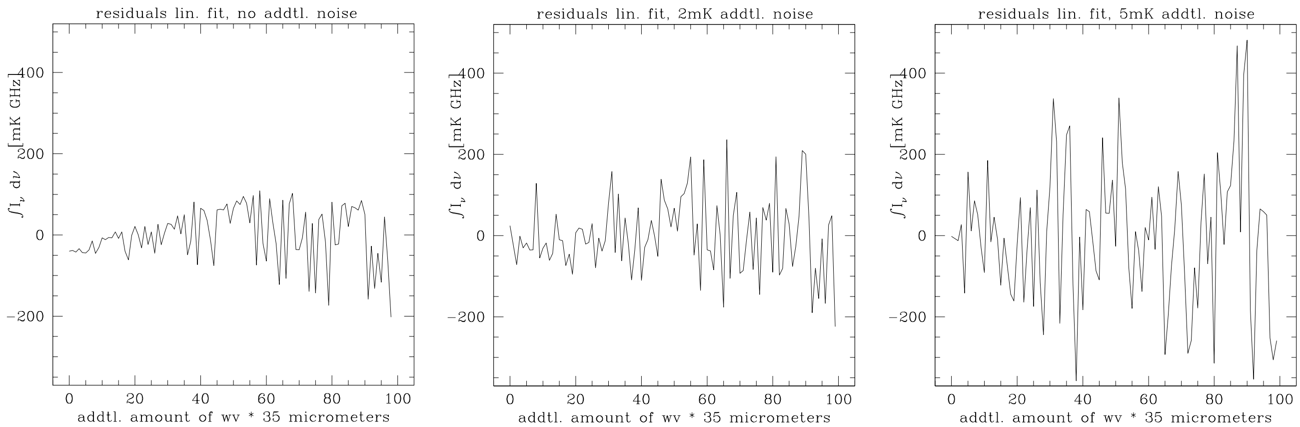

Figure 7. From left to right: Residuals from a linear fit to the data without noise which are shown in the right panel of Fig. 5 right, and from data with with 2 mK and 5mK rms noise which are shown in Fig. 6. The rms in the residuals for 2 mK rms noise (*center*) is dominated by the line shape effects which can be seen in the left frame. At 5 mK rms channel noise (*right*) the noise of the radiometer becomes dominant.

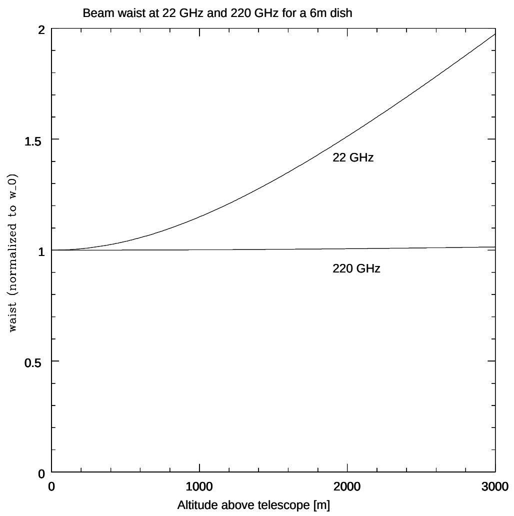

Figure 8. A comparison between the 22 GHz waist (top line) and the 220 GHz waist, of a 6 m dish, dependent on altitude above ground.

5. CONCLUSIONS

5.1. Choice of water vapor line

We conclude that the optical thin 22 GHz line is the best choice for monitoring phase delays due to atmospheric water vapor if the following conditions are satisfied:

a) The available radiometer is sufficiently sensitive to meet the derived requirements in the previous chapter. This means for the planned 32 channel lag correlator that each of its channels needs to have a rms noise temperature of not more than 2 mK.

b) The telescope site is not extremely dry (line of sight water vapor columns are not less than about 3 mm for the majority of time).

c) The altitude distribution of the excess water vapor is not confined to a thin layer in comparison to the 3 km uncertainty of altitude distribution assumed here.

If the above conditions are met, then the advantage of observing the 183 GHz line – its high brightness temperature – is overwhelmed by its high optical depth, and its higher sensitivity to the altitude of the water vapor and the total amount of water vapor. In particular the optical depths effects at total pwv greater than several mm will force observations further out in the line wings. Common line shape theories are unlikely to be accurate far out in the line wings and thus it is questionable whether a suitable observable can be defined.

5.2. Line shape fit versus linear combination of single channels

Line shape fitting leads to the best achievable accuracy for the determination of the path length deviations due to water vapor. The method provides the best achievable S/N ratio and is, to first order, insensitive to the altitude distribution of the additional layer of water vapor. Even when moderate optical depth effects are present, the method provides high accuracy result. At the moment we are exploring schemes to increase the achieved accuracy of this method, by choosing an observable other than just the integrated intensity of the fitted kinetic line shape. In this scheme we take into account the fitted line width. Another advantage of the line fit scheme is that it is flexible in terms of coping with improvements of the line shape theories, because the observable is derived from the fitted parameters of the corresponding line shape model.

The water vapor radiometer will provide best results if it has a large number of channels in order to allow a good fit of the line shape. Our design for a lag correlation receiver provides a 32 channel system with a total bandwidth of 6.5 GHz. It is based on an existing analog lag correlator and thus requires no additional developments. In this design we omit the very center of the line (the innermost 1.5 GHz) to simplify the hardware. This results in a higher sensitivity requirement, but this scheme is less sensitive to optical depth effects.

We conclude that the best suited radiometer for phase correction at the BIMA site of Hat Creek is a multi-channel radiometer for the 22 GHz water vapor line. For extremely dry sites with total pwv columns routinely less than 3mm, the 183 GHz line will be an excellent choice, too. A spectrometer similar to the one we propose to build would also be suitable for this line. How far off the line center a reliable line shape theory can be applied will determine the maximum amount of pwv for which the 183 GHz line actually can be used.

ACKNOWLEDGMENTS

We would like to thank D. Woody for many helpful discussions. We also like to thank E. Sutton, O. Lay, L. Mundy, and P. Teuben for their support and comments.

REFERENCES

Harris, A.I., Isaak, K.G., & Zmuidzinas, J., 1998, these proceedings

Marvel, K.B., Woody, D. P., 1998, these proceedings

McClatchey et al., 1972, *"Optical properties of the Atmosphere"*, 3rd edition, Air Force Cambridge Research
Laboratories Report AFCRL-72-0497, p. 93

Thompson, A.R., Moran, J.M. & Swenson, G.W., 1994, *"Interferometry and Synthesis in Radio Astronomy"*,Krieger
Publ., Malabar, Florida

Waters J.W., 1976, in: Meth. Exp. Phys. 12B, Meeks M.L. (ed.), 142-176